

THE FIRST STARS

DAVID ARNETT
Steward Observatory
University of Arizona
Tucson AZ 85721, USA

Abstract. The possible nature of the first generation of stars is considered, using a star of $25M_{\odot}$ as an example. General nucleosynthesis and the production of CNO catalysts is examined in detail. The increase in neutron excess and its significance for yields from explosive burning is discussed. An estimate of the ratio of ionizing photons to heavy elements produced is derived, for use in early universe simulations.

1. Introduction

The first stars are thought to produce the abundances seen in extreme population II objects, and the UV photons which re-ionize the universe (Gnedin & Ostriker, 1996). These stars are the culmination of an early epoch of structure formation, and may provide a new diagnostic tool for that era. They also bridge the gap between cosmological nucleosynthesis and the stellar nucleosynthesis currently seen.

2. Preliminary Considerations

2.1. INITIAL ABUNDANCES

The pattern of cosmological nucleosynthesis gives an interesting concordance (Wagoner, Fowler, & Hoyle, 1968; Schramm & Wagoner, 1979; Kolb & Turner, 1990) between predicted and inferred abundances of D, ^3He , ^4He , and ^7Li . Figure 1 shows this abundance pattern in more detail, as it appears upon re-calculation. The abundances are usually presented for those values above 10^{-12} , which is shown as a dotted line; here the lower limit is extended to 10^{-18} . The new nuclei are ^7Li , ^9Be , ^{10}B , ^{11}B , ^{12}C , ^{13}C , ^{14}C , and ^{14}N . All other nuclei are rarer. The total abundance of potential

catalysts for CNO burning is $X(\text{CNO}) \approx 10^{-14}$. As we shall see, these levels of abundance are inadequate for stable hydrogen burning.

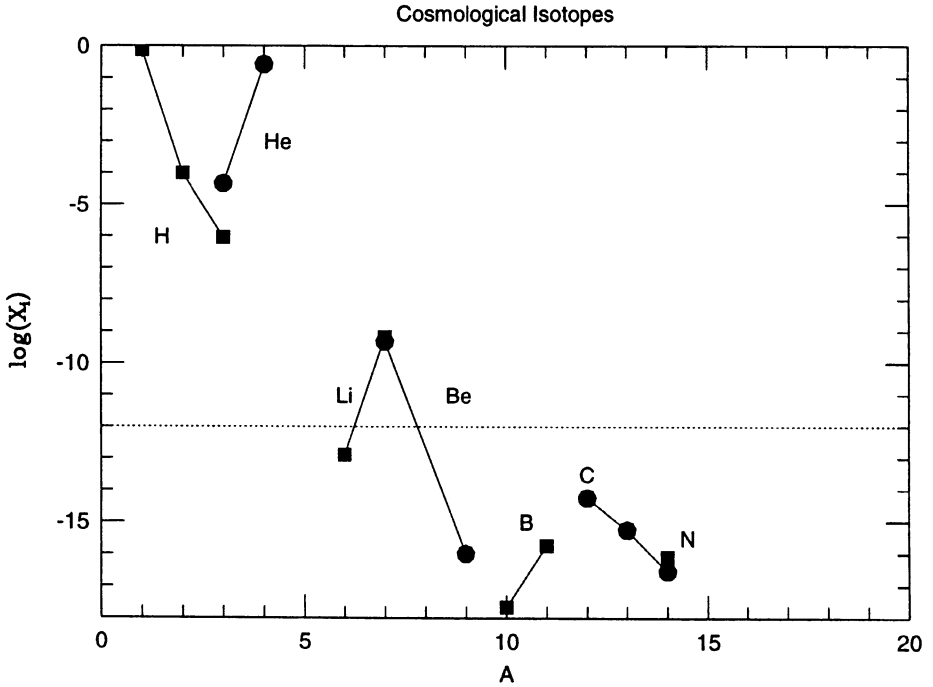


Figure 1. Cosmological Abundances.

2.2. REACTION NETWORK

While this recalculation of Big Bang nucleosynthesis used a network typical of previous work, a larger network was necessary for exploring subsequent nucleosynthesis. This network is shown in Figure 2; it contains 238 nuclei. The solid squares denote stable isotopes; the open squares are isotopes which are radioactive.

3. Failure of the pp-chain

An important feature of the evolution of the first stars is that, with the absence of CNO catalysts, the massive stars do not burn hydrogen under conditions of thermal balance. This may be simply shown. Following

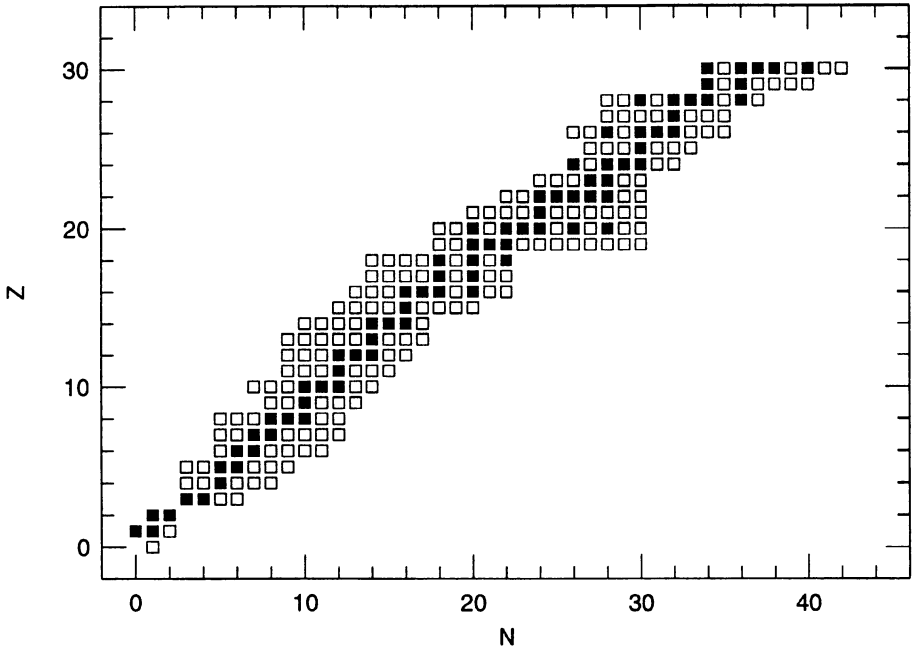


Figure 2. Nuclear Reaction Network.

Eddington, (see (Arnett, 1996) for detailed discussion),

$$L/M = 4\pi cG(1 - \beta)/\kappa, \tag{1}$$

where β , the ratio of gas to total pressure, may be related to radiation entropy per nucleon, $S_\gamma = \frac{4}{3}aT^3/N_A k\rho$, by

$$1 - \beta = S_\gamma/(S_\gamma + 4Y), \tag{2}$$

where Y is the total number of ideal gas particles per nucleon (ionized electrons plus ions).

For massive stars, which both produce ionizing radiation and synthesize new elements, the opacity κ is essentially just the Thomson scattering value, and $S_\gamma \approx 1$ for a star of $25 M_\odot$. For a Salpeter initial mass function, such a mass corresponds to the typical star for bulk nucleosynthesis.

For Big Bang abundances ($X_H = 0.77$, and $X_{He} = 0.23$), this gives

$$L/M = 9.3 \times 10^3 \text{ erg g}^{-1}\text{s}^{-1}. \tag{3}$$

$T/10^8$ K	$\rho/(10^2\text{g/cc})$	$\epsilon(pp)$ erg/g s	$\epsilon(CNO)$ erg/g s	$\epsilon(3\alpha)$ erg/g s
0.50	0.15	3.2E+02	7.6E-05	1.5E-09
0.57	0.23	6.6E+02	6.8E-04	9.2E-08
0.66	0.35	1.4E+03	5.5E-03	4.8E-06
0.76	0.53	2.7E+03	4.2E-02	2.1E-04
0.87	0.80	5.4E+03	2.9E-01	7.6E-03
1.00	1.20	1.0E+04	1.9E+00	2.4E-01
1.15	1.82	2.0E+04	1.1E+01	6.8E+00
1.32	2.76	3.8E+04	6.4E+01	1.9E+02
1.51	4.18	7.1E+04	3.4E+02	7.6E+03
1.73	6.32	1.3E+05	1.7E+03	3.4E+05
1.99	9.57	2.4E+05	8.1E+03	1.2E+07

TABLE 1. Energy generation rates for $M = 25M_{\odot}$ ($S_{\gamma} = 1$).

For thermal balance, in which the energy radiated is replaced by energy from nuclear burning, $\langle \epsilon \rangle = L/M$. This gives a constraint on the energy release necessary for stable burning.

This may be compared with the actual energy generation rates from the pp-chain, the CNO cycle, and the triple-alpha process, which are given in Table 1. The rates are not drastically different from classical estimates (Clayton, 1968). We see that temperature of order 10^8 K are needed to attain thermal balance by the pp-chain, $\langle \epsilon(pp) \rangle \approx 10^4$. This is shown in the third column. The fourth column gives the CNO energy generation rate, using the Big Bang value of $X(CNO) \approx 10^{-14}$. Despite its more sensitive dependence upon temperature, the CNO rate is smaller than the pp-chain rate throughout the temperature range shown. In the last column is given the energy generation rate for helium burning by the triple-alpha reaction, $\epsilon(3\alpha)$, which exceeds $\epsilon(pp)$ for temperatures $T > 1.7 \times 10^8$ K. The time scale for thermal cooling is $\tau_{thermal} = E/\epsilon \approx 1.5 \times 10^{12}$ s. These features have implications for the evolution of the star.

The time for consumption of hydrogen is $\tau_H = -X_H / (dX_H/dt)$, which is given in Table 2. The rate of energy generation by the CNO cycle is proportional to the abundance of catalyst nuclei available,

$$\epsilon_{CNO} = X(CNO)X(H)f(\rho, T). \quad (4)$$

For what catalyst abundance $X(CNO)$, does $\epsilon(CNO)$ balance the energy loss by radiation, $L/M \approx 10^4$ erg/g s? This is denoted by $X(CNO)$ in Table 2. For abundance of catalysts appropriate to the Big Bang, $X(CNO) \approx 10^{-14}$, the star would have to reach temperatures $T \approx 2 \times 10^8$ K to balance radiation loss by CNO burning.

$T/10^8$ K	$\rho/10^2$ (g/cc)	τ_H (s)	$X(CNO)$	$\Delta X(CNO)$
0.50	0.15	1.7E+16	1.3E-06	1.3E-15
0.57	0.23	8.2E+15	1.5E-07	8.0E-14
0.66	0.35	4.0E+15	1.8E-08	4.1E-12
0.76	0.53	2.0E+15	2.4E-09	1.8E-10
0.87	0.80	1.0E+15	3.5E-10	6.6E-09
1.00	1.20	5.1E+14	5.3E-11	2.1E-07
1.15	1.82	2.7E+14	8.8E-12	6.2E-06
1.32	2.76	1.4E+14	1.6E-12	2.3E-04
1.51	4.18	7.6E+13	2.9E-13	1.4E-02
1.73	6.32	4.2E+13	5.8E-14	7.8E-01
1.99	9.57	2.3E+13	1.2E-14	3.0E+01

TABLE 2. Burning Parameters for $M = 25M_{\odot}$ ($S_{\gamma} = 1$).

Suppose the star contracts on a timescale $\tau_{thermal}$ to $T \approx 10^8$ K where $\langle \epsilon \rangle \approx L/M$. During this time the triple alpha reaction would increase the abundance of CNO by

$$\Delta X(CNO) \approx \frac{dX(3\alpha)}{dt} \tau_{thermal}. \quad (5)$$

This crude estimate suggests that as the star approaches thermal balance by the pp-chain, the triple alpha process enhances the abundance of CNO catalysts by a sufficient amount to allow CNO cycle burning to take over.

4. Nucleosynthesis

4.1. TO THE END OF HYDROGEN BURNING

Figure 3 shows the detailed evolution of abundances using the network of Figure 2. The lower panel displays the logarithm of the abundance (nucleon fraction) versus time. The upper panel shows the evolution of the energy generation rate ϵ , the radiation loss L/M , and the neutrino cooling s_{ν} (here near zero).

The cosmological abundance by number of D and ^3He are comparable to that of CNO catalysts in Population II stars, so that the burning of these isotopes to carbon would help solve the problem of the deficiency of catalysts. The first stage of burning destroys D, and converts some ^7Be to ^7Li ; this causes a rapid thermal adjustment (not shown).

Then a steady increase in temperature begins, in which all the light nuclei (below ^{12}C) are destroyed, excepting only H and ^4He . Essentially none of these nuclei become potential catalysts; they burn to ^4He . This causes the weak “blip” in ϵ at $t \approx 3 \times 10^{11}$ s.

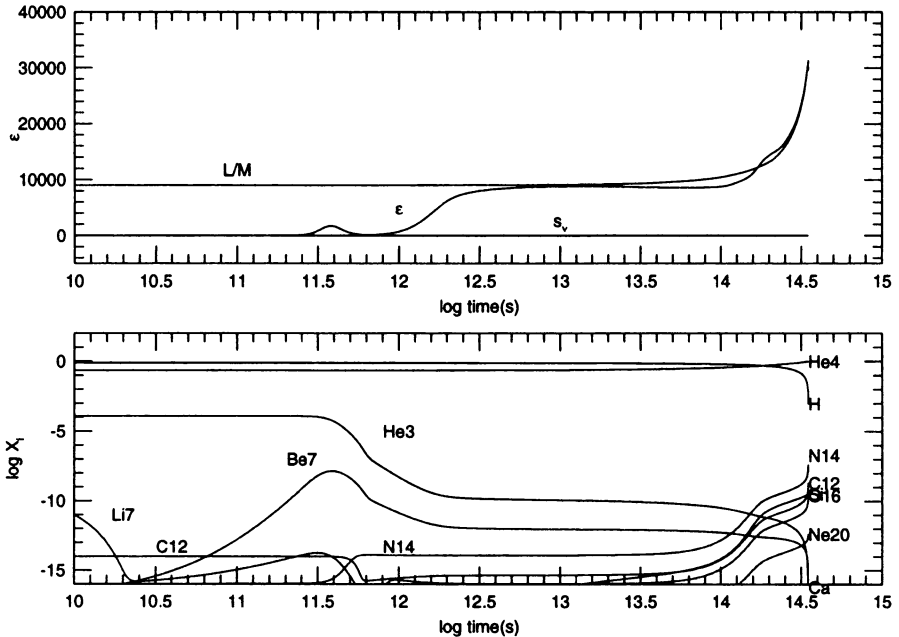


Figure 3. Evolution of Abundances ($S_7 = 1$).

4.2. FORMATION OF CNO CATALYSTS

As suggested by the simple analysis above, when the temperature approaches 10^8 K, the triple-alpha reaction begins to produce ^{12}C , which begins a high temperature CNO cycle. Note the rapid rise of ^{14}N , ^{12}C , and ^{16}O , in Figure 3. More surprising is the rise of Si isotopes, which approach a nucleon fraction of 10^{-9} .

The burning proceeds steadily at these temperatures, consuming hydrogen. The abundances after hydrogen burning are shown in Figure 4. Stable nuclei are shown as solid symbols, radioactive by open ones. After ^1H and ^4He , ^{14}N is most abundant, with a nucleon fraction $\approx 10^{-7}$ (the solar abundance of this nucleus is about 10^{-3}). In this high temperature hydrogen burning, proton reactions produce nuclei up to Ar, although their abundance is low (10^{-9}). Several radioactive nuclei are produced (^{13}N , ^{14}O , ^{15}O , ^{17}F , ^{18}F , ^{22}Na , and ^{26}Al).

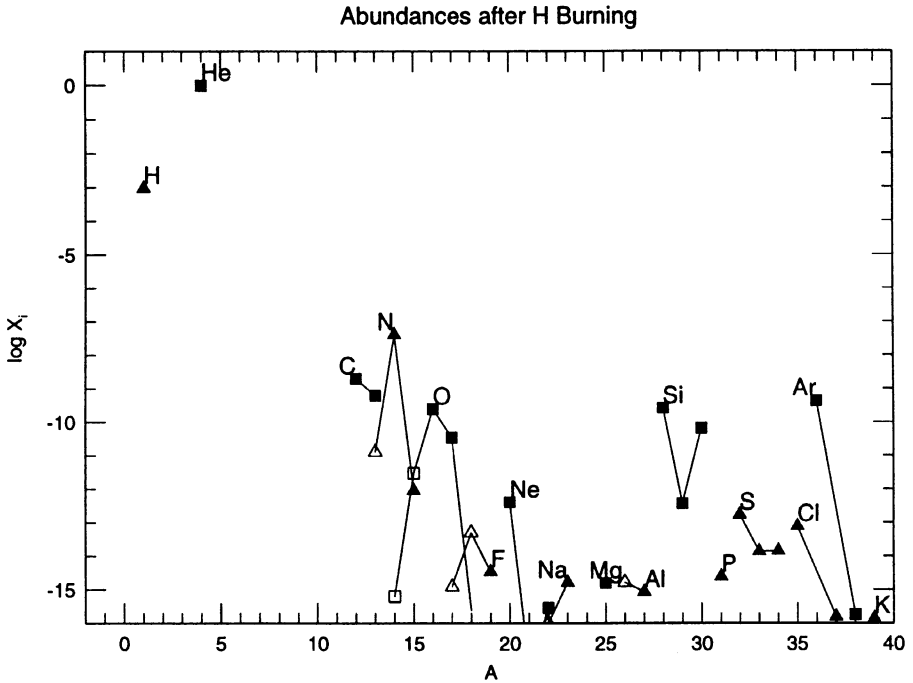


Figure 4. Abundances after Hydrogen Burning.

4.3. CHANGE IN NEUTRON EXCESS

When the H abundance falls below about 10^{-4} , helium burning begins to dominate, producing more ^{12}C and ^{16}O , and some ^{20}Ne as helium begins to be depleted.

With the onset of carbon burning, the production of free protons drives production of ^{14}N , which is then consumed as more massive nuclei are formed. Even at the onset of neon burning, the abundance of iron peak nuclei is tiny: only 10^{-21} or so.

The neutron excess $\eta = (N - Z)/A$ rises steadily during carbon burning. For the solar abundance pattern the neutron excess is $\eta_{\odot} \approx 1.5 \times 10^{-3}$. For Population II it is smaller by about a factor of 10^{-2} , or $\eta_{\text{pop.II}} \approx 1.5 \times 10^{-5}$. At the beginning of carbon burning, $\eta = 1.0 \times 10^{-7}$, and increases to $\eta = 3.5 \times 10^{-4}$ at carbon consumption.

In explosive carbon burning, the abundance of ^{23}Na or ^{27}Al relative to ^{20}Ne or ^{24}Mg is proportional to η (Arnett, 1971). This, along with the contribution to Na and Al production from high temperature hydrogen shell

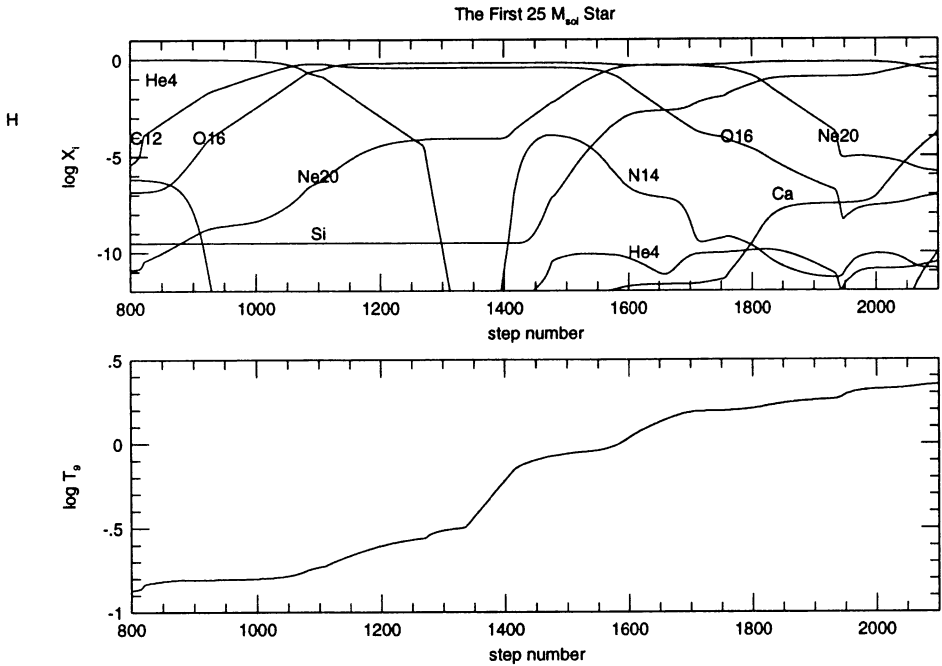


Figure 5. Further Changes in Abundances.

burning, may dominate the most extreme Population II abundances of these elements. If this were the dominant effect, it would imply a deficiency of (Na,Al) to (Ne,Mg) of only a factor of one-fourth.

Hydrostatic neon burning increases η further, to about 5×10^{-4} , or roughly one-third solar. Such layers are oxygen rich, and may undergo explosive oxygen burning. To the extent that most of the neutron excess lies in nuclei with two excess neutrons, such as ^{34}S and ^{38}Ar , the number of neutrons scales as $\sqrt{\eta}$. In quasiequilibrium (explosive oxygen or silicon burning) this causes the ratios of odd/even elements also to scale as $\sqrt{\eta}$. If this were the dominant effect, these ratios would be only about 0.58 solar, which is an interesting notion to test observationally in extreme Population II stars.

5. Production of Ionizing Radiation and Metals

Because essentially the same stars are involved, there is a close connection between the production of ionizing radiation, and the production of carbon and heavier elements (“metals”). This discussion is based upon the formu-

lation in (Arnett, 1996); a critical discussion of the initial mass function (IMF) may be found there.

The total mass burned from hydrogen into helium, for stars from 20 to $100M_{\odot}$, is

$$M_{\alpha}(20, 100) = 0.168\xi_0 X_H, \quad (6)$$

for a Salpeter IMF (the simplest choice). Here ξ_0 is a normalizing constant which can be estimated for the solar neighborhood; it will cancel below. The average energy of photons radiated in the mass range is $\langle h\nu \rangle = f I_H$, where $I_H = 13.6$ eV. Burning H to He releases $Q = 7$ MeV per nucleon consumed. The total mass of metals produced and returned to space by core collapse supernovae is

$$M_{COej} = 0.926\xi_0. \quad (7)$$

The ratio of the number of ionizing photons to the number of heavy elements produced in massive stars is then

$$N_{ion}/N_z = 1.81(X_H Q A)/(f I_H), \quad (8)$$

where $A \approx 16$ is the mean atomic weight of the heavy elements. This becomes

$$N_{ion}/N_z = 1.5 \times 10^7 / f. \quad (9)$$

The primary uncertainty may lie in f , which depends upon details of evolution in the HR diagram and mass loss. Several simple attempts at variations in the IMF tended to cancel, leaving this ratio only slowly varying. This estimate may be of value in simulations of the early universe (Gnedin & Ostriker, 1996).

6. Conclusions

This discussion has focused on relatively robust results, that could be simply derived. More detailed stellar evolutionary sequences (one dimensional) were found to be sensitive to the details of convective mixing. Given the results of direct two dimensional simulations of late stellar evolution (Bazan & Arnett, 1998), this is not surprising. A better understanding of stellar mixing will be needed to provide reliable detailed predictions of nucleosynthesis yields. Direct experimental tests (Remington, Weber, Marinak, et al., 1995; Kane, Arnett, & Remington, 1997) of the numerical simulation methods are beginning to give a more secure basis for extended extrapolations of this kind.

7. Acknowledgements

The suggestion of Prof. J. P. Ostriker on the importance of the ratio of production of ionizing radiation to metals is gratefully acknowledged. This work has been supported in part by the National Aeronautics and Space Administration grant NAGW-2798 and National Science Foundation grant AST94-17346.

References

- Arnett, D., *Astrophys. J.* **166**, 153, 1971,
Arnett, D., *Supernovae and Nucleosynthesis*, Princeton: Princeton University Press, 1996.
Bazan, G. & Arnett, D., *Astrophys. J.*, 1998, in press.
Clayton, D. D., 1968, *Principles of Stellar Evolution and Nucleosynthesis*, McGraw-Hill, New York.
Gnedin, N., & Ostriker, J. P., *Astrophys. J.* **484**, 581, 1996.
Kane, J., Arnett, D., Remington, B., et al., 1997, *Astrophys. J. Letters*, in press.
Kolb, E. W., & Turner, M. S., 1990, *The Early Universe*, Addison-Wesley, Reading, MA.
Remington, B. A., Weber, S. V., Marinak, M. M., et al., *Phys. Plasmas* **2**, 241, 1995.
Schramm, D. N., & Wagoner, R. V., 1979, *Ann. Rev. Nucl. Part. Sci.* **27**, 37.
Wagoner, R. V., Fowler, W. A., & Hoyle, F., 1967, *Astrophys. J.* **148**, 3.